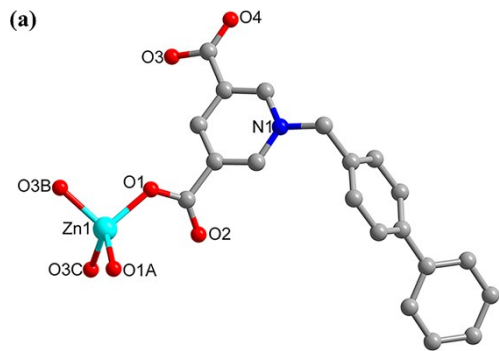


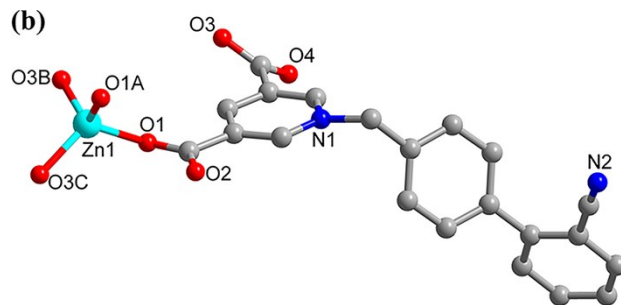
Supporting Information

Computational Descriptions

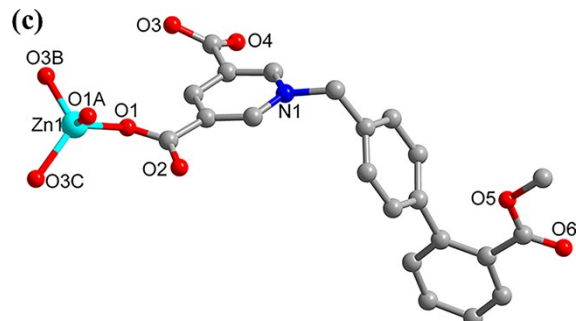
Within the framework of density functional theory, the electronic structure properties for 1, 2 and 3 were simulated using the Vienna ab initio simulation package (VASP).¹ The Perdew-Burke-Ernzerhof functional with the generalized gradient approximation (PBE-GGA) was used for electron exchange-correlation, and the projector-augmented-wave (PAW) method were adopted to describe the inert core electrons.^{2,3} A kinetic energy cutoff of 400 eV and a gamma-centered k-point grid of $4 \times 4 \times 2$ were used for all calculations. The valence electron for each element is Zn 4s²3d¹⁰, C 2s²2p², O 2s²2p⁴, N 2s²2p³ and H 1s¹. In addition, the DFT-D3 dispersion correction method of Grimme et al. was considered because of the weak interactions found in systems.⁴ Starting with the X-ray crystal data, the lattice parameters and the atomic positions were fully relaxed until the energy difference is less than 10^{-5} eV and the force is smaller than 10^{-2} eV/ Å. The calculated results of the electronic band structure and density of states were treated by the powerful high throughput analysis software, VASPKIT.⁵



Symmetry codes: A = 1 - x, y, 1/2 - z; B = 1 - x, 3-y, 1-z; C = x, 3 - y, -1/2 + z.



Symmetry codes: A = 1 - x, y, 3/2 - z; B = 1 - x, 2-y, 1-z; C = x, 2 - y, 1/2 + z.



Symmetry codes: A = 1 - x, y, 3/2 - z; B = 1 - x, 2 - y, 1 - z; C = x, 2 - y, 1/2 + z.

Figure S1. The coordination environments of Zn(II) cations of (a) **1**, (b) **2**, and (c) **3**. All H atoms are omitted for clarity.

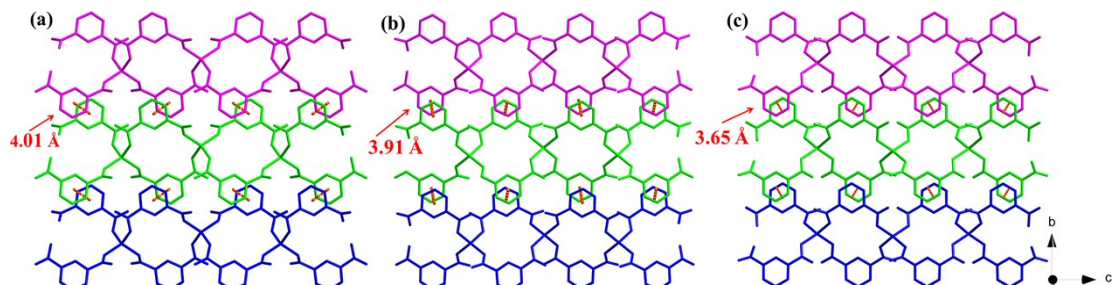


Figure S2. Representations viewed along a-axis of the centroid-to-centroid distance of adjacent pyridine rings for (a) **1**, (b) **2**, and (c) **3**. The biphenyl rings are omitted for clarity.

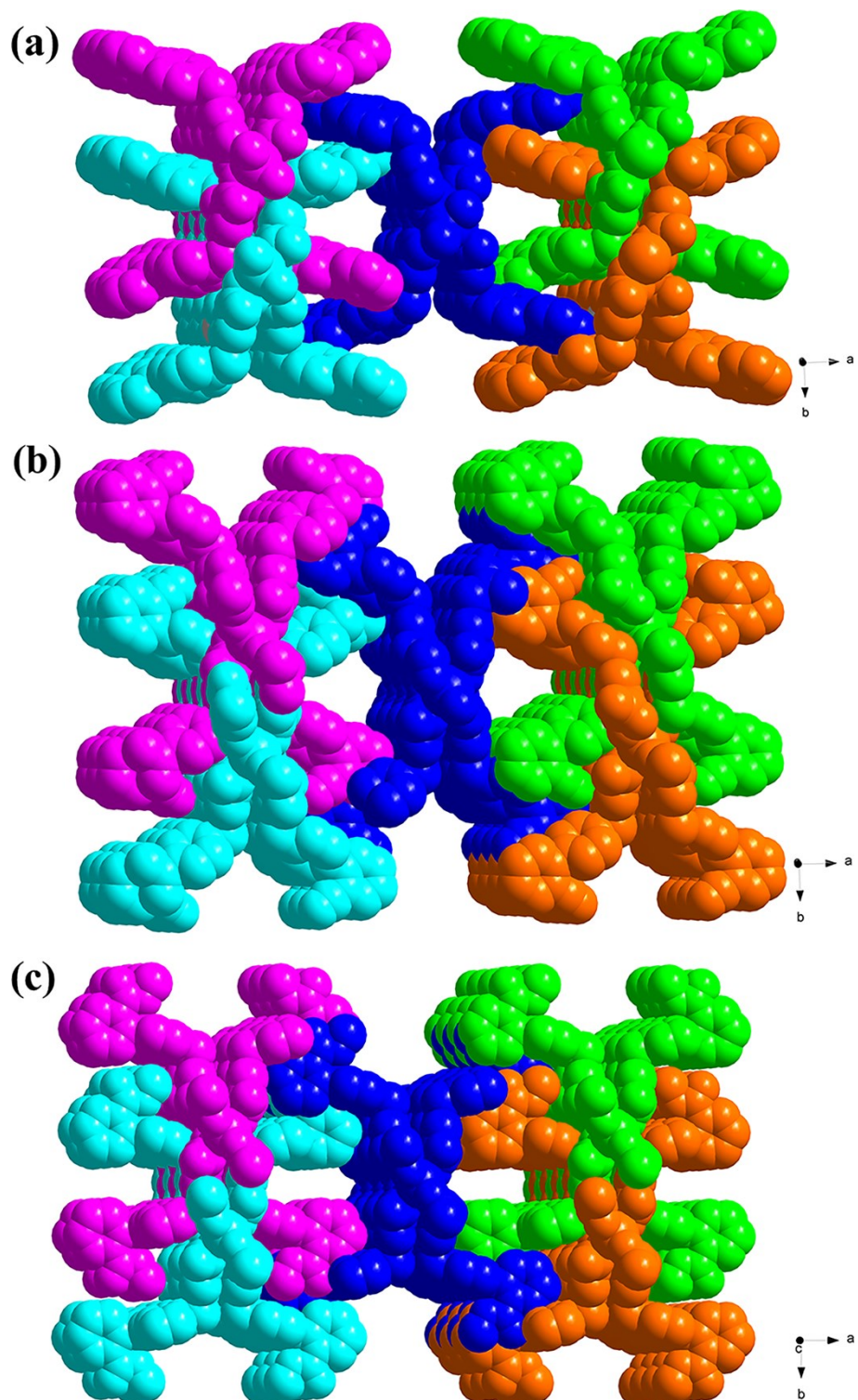


Figure S3. Three-dimension supramoleculars of (a) **1**, (b) **2**, and (c) **3** in space-filling modes.

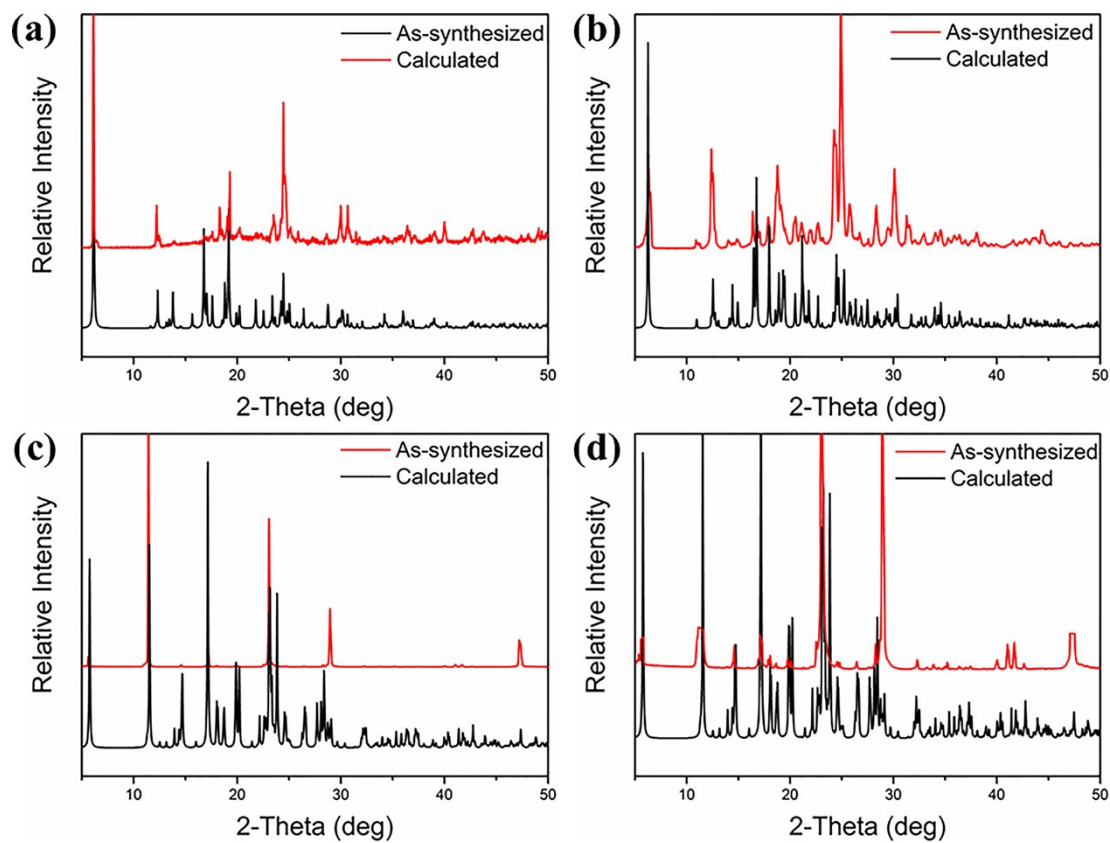


Figure S4. As-synthesized and calculated PXRD patterns of (a) 1, (b) 2, and (c) 3, (d) because some peaks are too strong to cover other peaks, we deleted data over a certain intensity of (c).

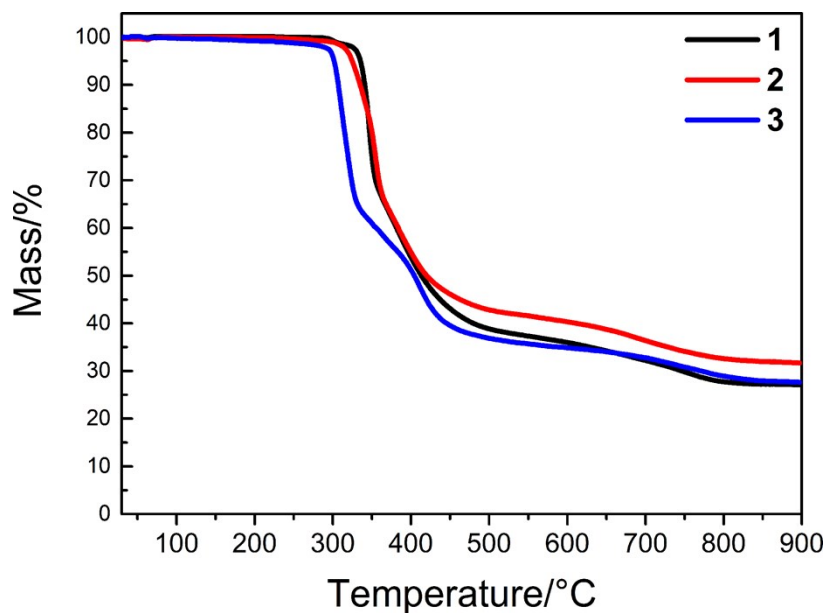


Figure S5. The TGA curves of 1 - 3.

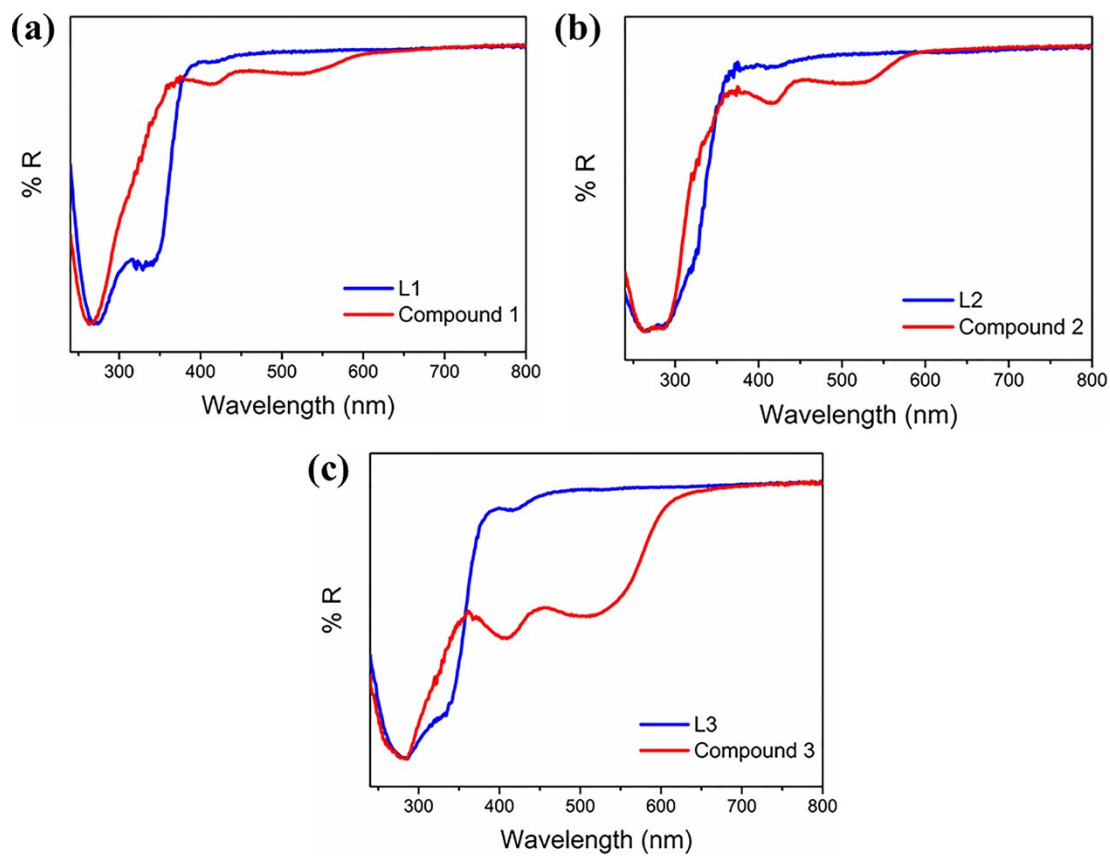


Figure S6. UV-vis spectra of (a) L1 and **1**, (b) L2 and **2**, and (c) L3 and **3** (Y-axis has been normalized to [0, 1]).

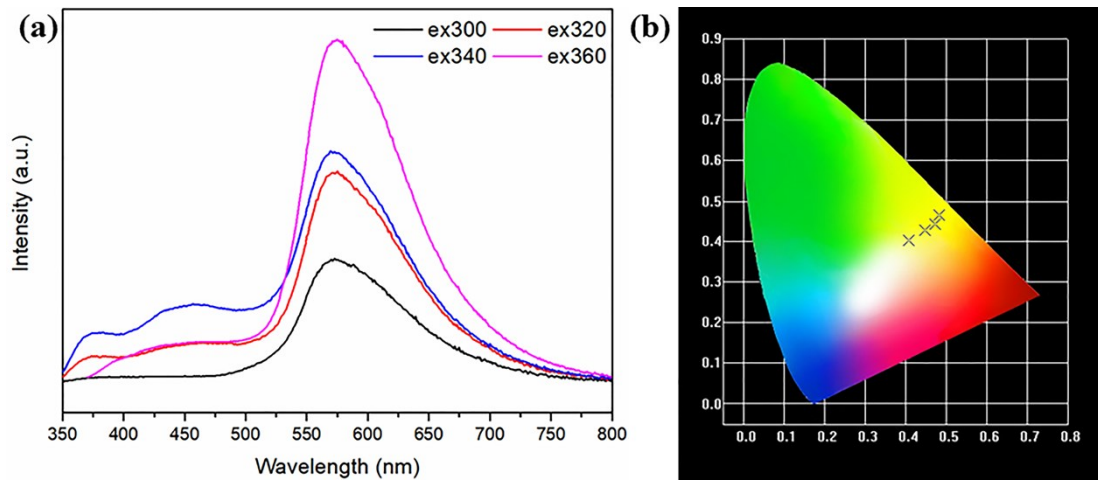


Figure S7. (a) Solid state emission spectra of **2** by variation of excitation wavelengths at 298K, (b) CIE-1931 chromaticity diagram of the emission spectra corresponding to (a).

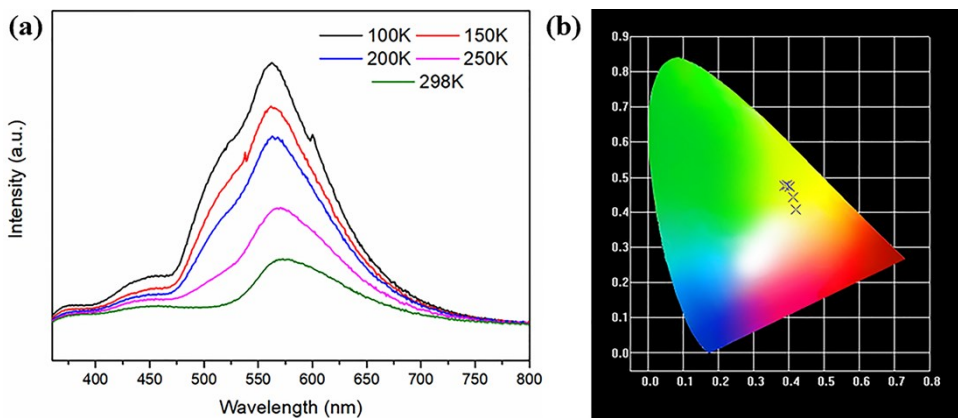


Figure S8. (a) Solid state emission spectra of **2** with different temperature under an excitation of 340 nm, (b) CIE-1931 chromaticity diagram of the emission spectra corresponding to (a).

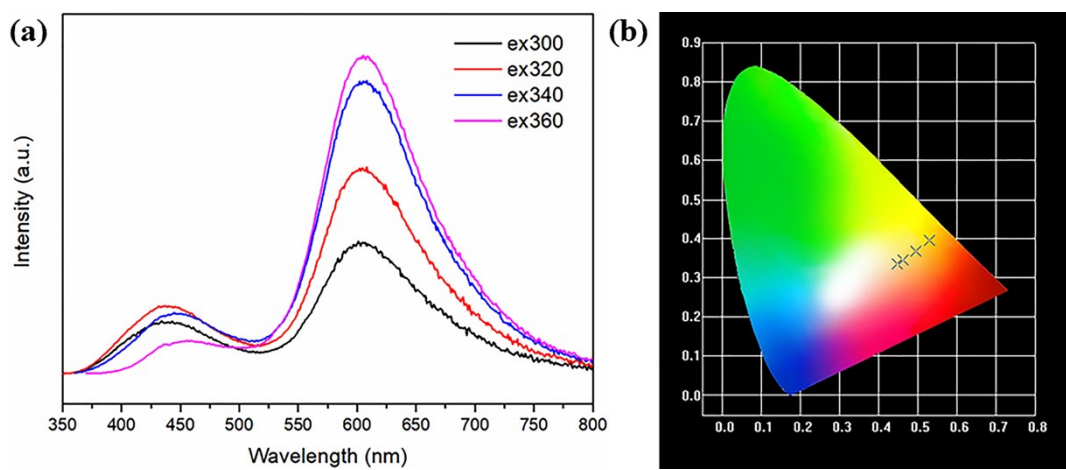


Figure S9. (a) Solid state emission spectra of compound **3** by variation of excitation light at 298K, (b) CIE-1931 chromaticity diagram of the emission spectra corresponding to (a).

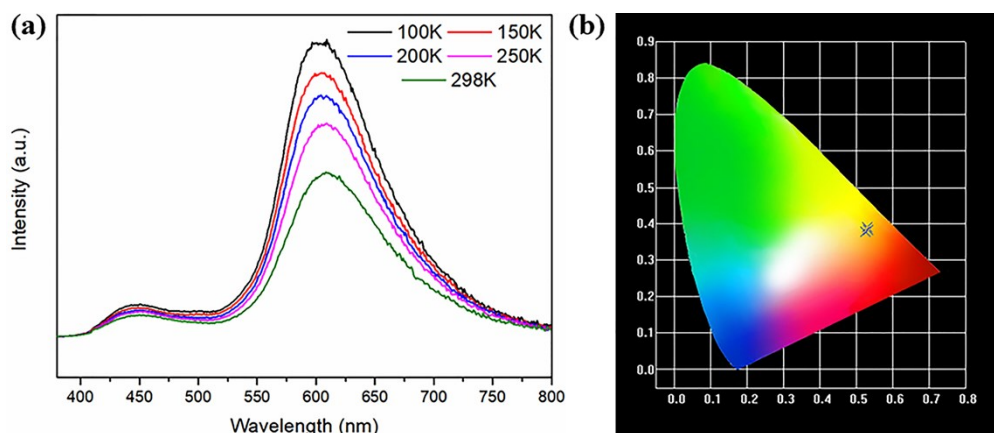


Figure S10. (a) Solid state emission spectra of **3** with different temperature under an excitation of 360 nm. (b) CIE-1931 chromaticity diagram of the emission spectra corresponding to (a).

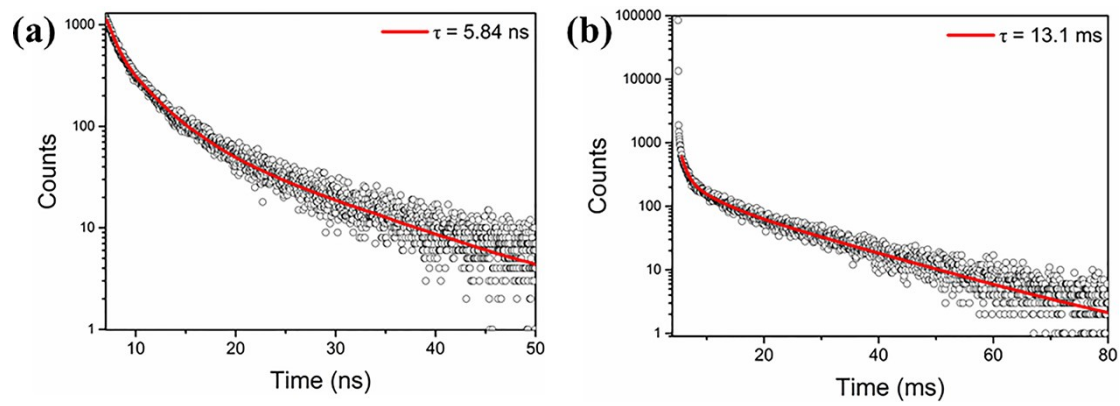


Figure S11. PL decay curves of **1** (a) with excitation at 375 nm and the emission peaks at 420 nm, (b) with excitation at 350 nm and the emission peaks at 580 nm in solid state at room temperature.

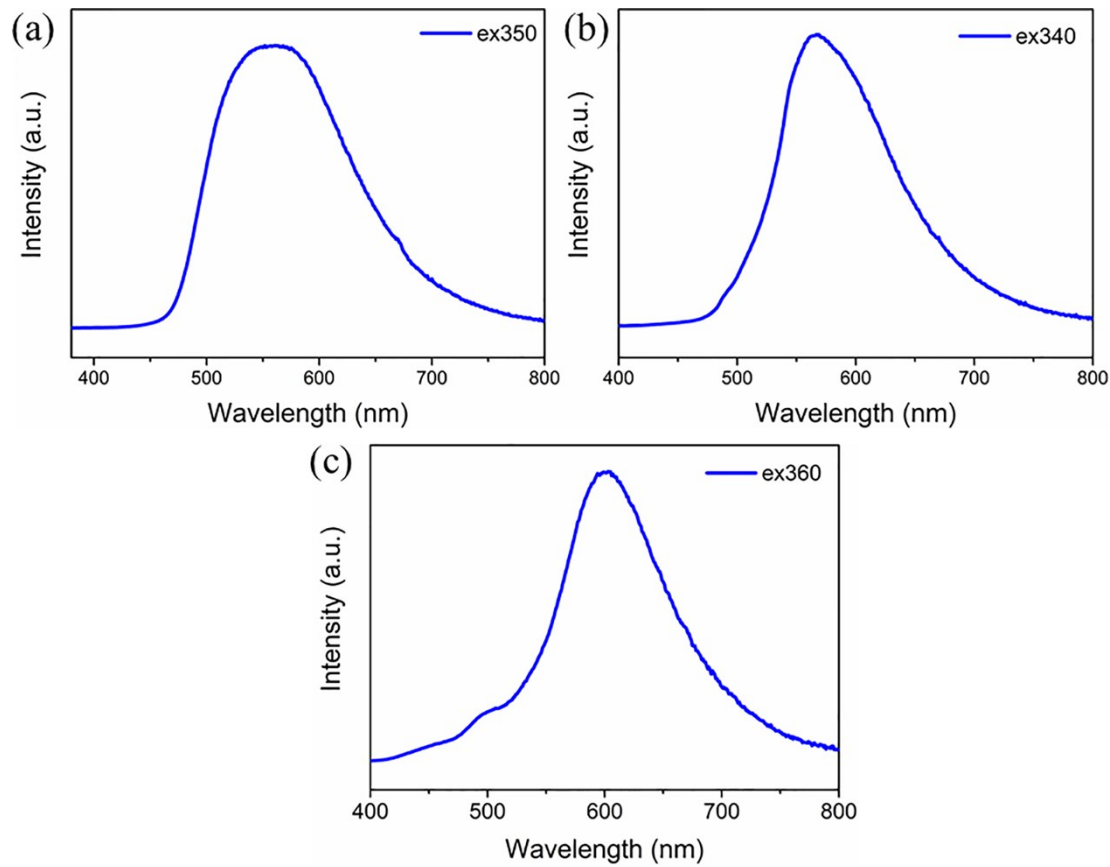


Figure S12. Phosphorescence spectra recorded at room temperature of (a) **1**, (b) **2** and (c) **3** with a delay time in the range of 1000-200000 μ s.

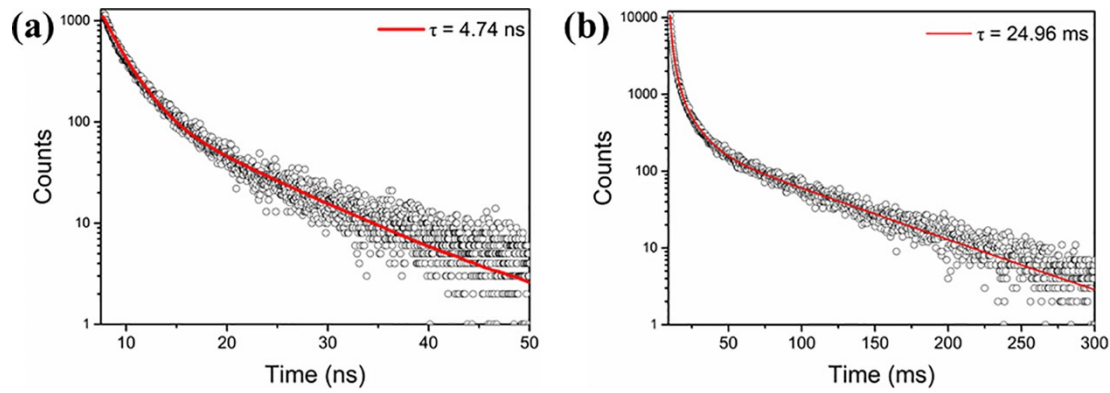


Figure S13. PL decay curves of **2** (a) with excitation at 375 nm and the emission peaks at 450 nm, (b) with excitation at 340 nm and the emission peaks at 570 nm in solid state at room temperature.

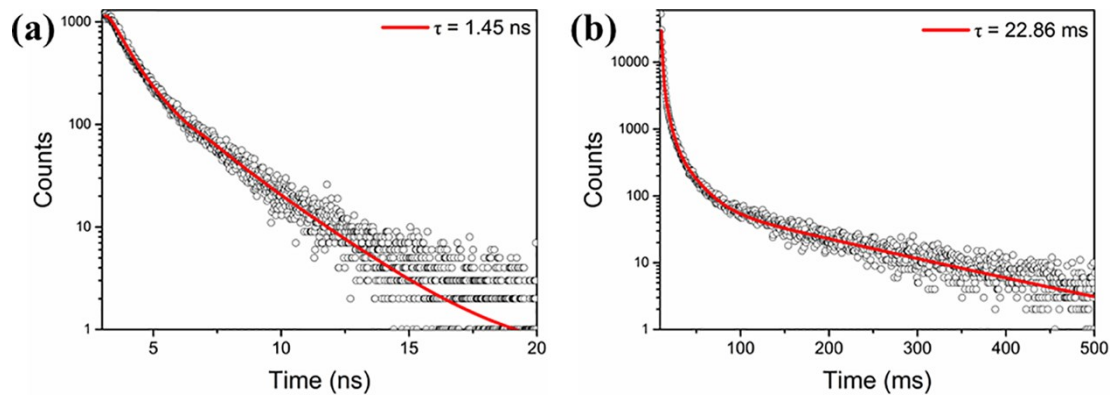


Figure S14. PL decay curves of **3** (a) with excitation at 375 nm and the emission peaks at 450 nm , (b) with excitation at 360 nm and the emission peaks at 605 nm in solid state at room temperature.

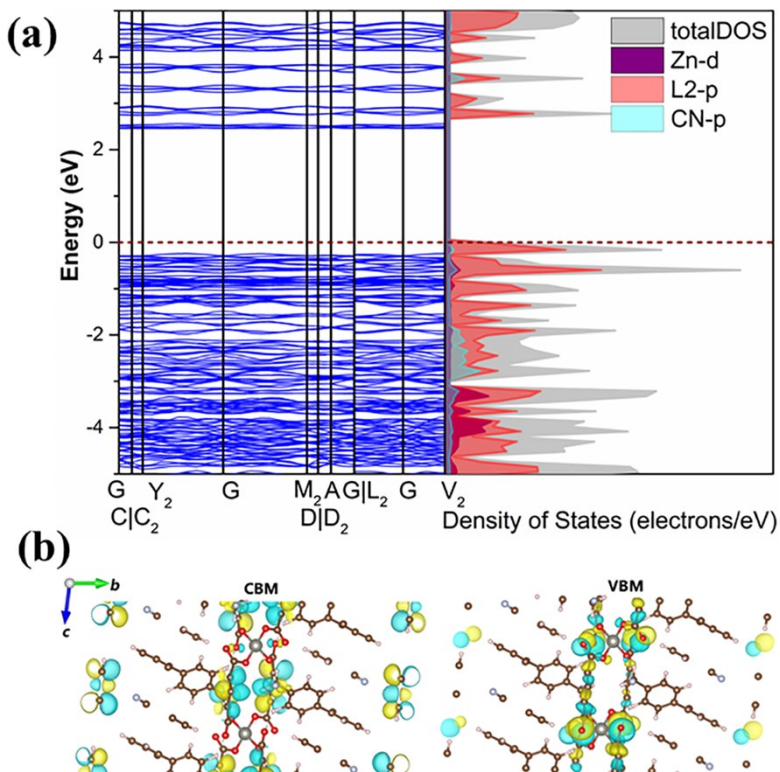


Figure S15. Calculated electronic structure properties of **2**. (a) Calculated band structure and projected density of states. (b) Calculated charge densities of the CBM and VBM.

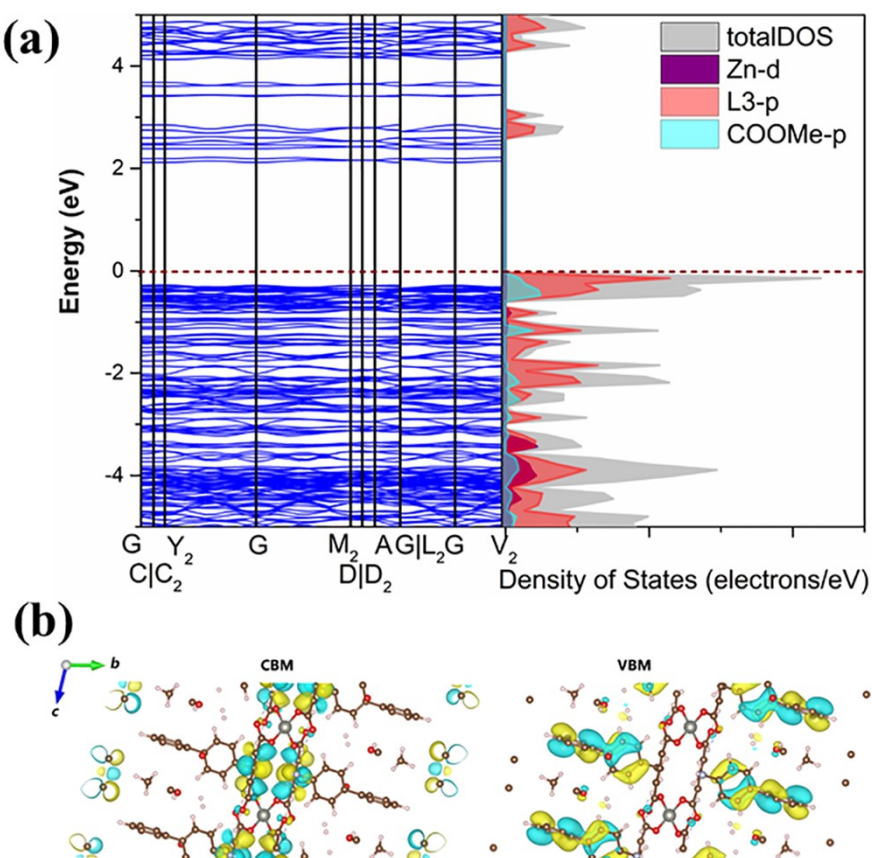
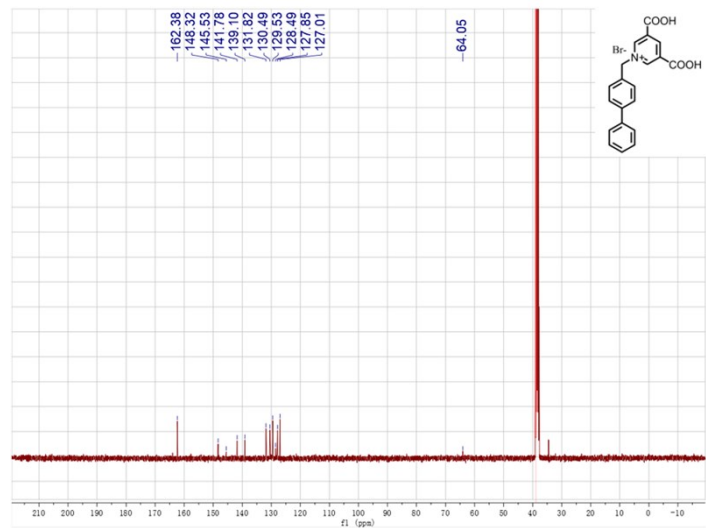
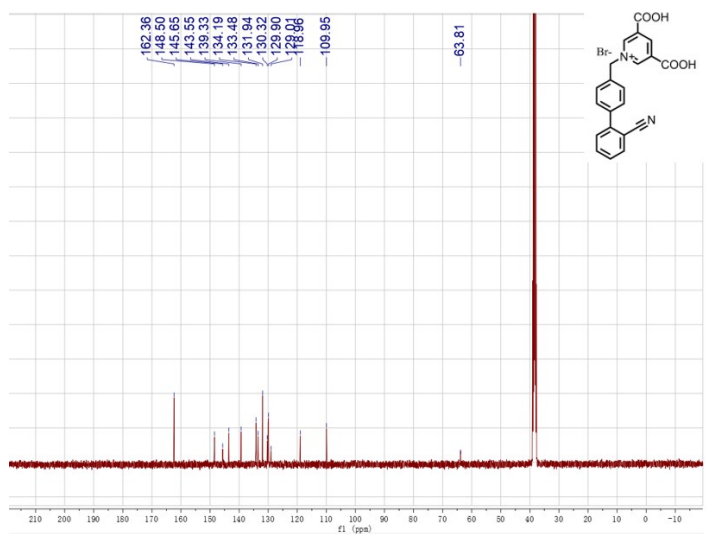


Figure S16. Calculated electronic structure properties of **3**. (a) Calculated band

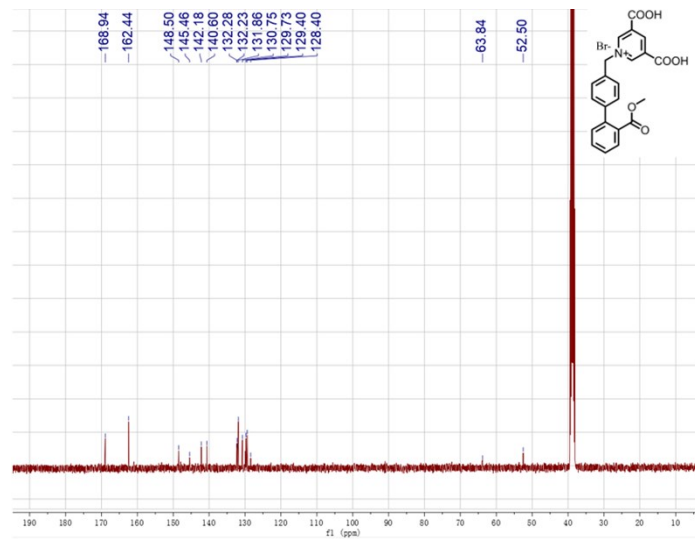
structure and projected density of states. (b) Calculated charge densities of the CBM and VBM.



L1 (100 MHz, DMSO-d₆)



L2 (100 MHz, DMSO-d₆)



L3 (100 MHz, DMSO-d₆)

Figure S17. ¹³C NMR spectra for L1–L3.

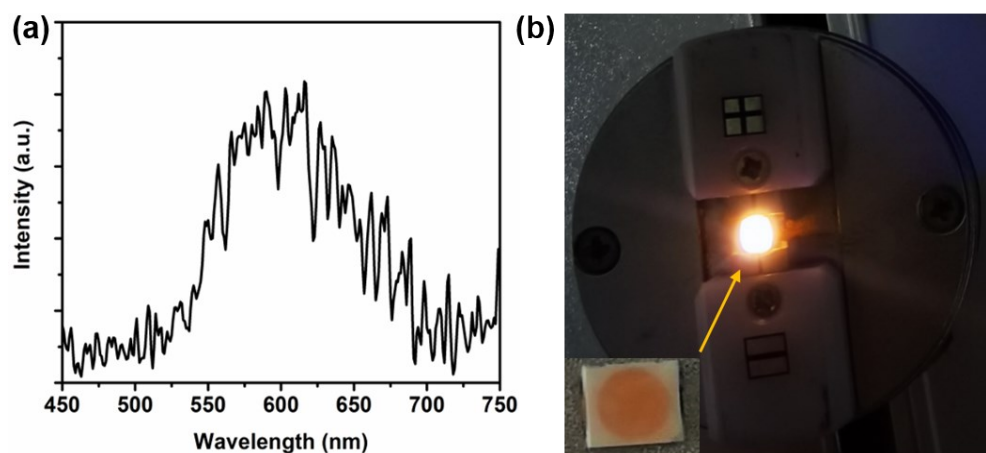


Figure S18. The LED fabrication and performance test. (a) the PL spectra corresponding to the LED. (b) The photograph of the LED.

Table S1. Crystal data and structure refinements for 1–3.

Identification code	1	2	3
Empirical formula	C ₄₀ N ₂ O ₈ Zn	C ₄₂ H ₂₆ N ₄ O ₈ Zn	C ₄₄ H ₃₂ N ₂ O ₁₂ Zn
Formula weight	701.85	780.04	846.08
Temperature/K	150	150	150
Crystal system	monoclinic	monoclinic	monoclinic
Space group	<i>C</i> 2/ <i>c</i>	<i>C</i> 2/ <i>c</i>	<i>C</i> 2/ <i>c</i>
<i>a</i> /Å	28.7233(13)	28.4195(4)	31.2645(7)
<i>b</i> /Å	7.8826(3)	8.40750(10)	8.0713(2)
<i>c</i> /Å	14.5754(5)	14.5457(2)	14.8768(3)
<i>α</i> /°	90	90	90
<i>β</i> /°	91.791(4)	96.8570(10)	103.092(2)
<i>γ</i> /°	90	90	90
Volume/Å ³	3298.5(2)	3450.65(8)	3656.51(15)
<i>Z</i>	4	4	4
<i>ρ</i> _{calc} g/cm ³	1.4132	1.501	1.537
<i>μ/mm⁻¹</i>	0.803	0.996	1.013
<i>F</i> (000)	1394.0	1600.0	1744.0
Radiation	MoKα ($\lambda = 0.71073$)	GaKα ($\lambda = 1.3405$)	GaKα ($\lambda = 1.3405$)
2θ range for data collection/°	7.2 to 59.3	9.544 to 121.178	5.046 to 121.396
Index ranges	-38 ≤ <i>h</i> ≤ 38, -10 ≤ <i>k</i> ≤ 10, -36 ≤ <i>h</i> ≤ 36, -10 ≤ <i>k</i> ≤ 8, -18 ≤ <i>l</i> ≤ 20	-39 ≤ <i>h</i> ≤ 40, -9 ≤ <i>k</i> ≤ 10, -18 ≤ <i>l</i> ≤ 18	-11 ≤ <i>l</i> ≤ 19
Reflections collected	11352	14275	15479
Independent reflections	4035 [<i>R</i> _{int} = 0.0251, <i>R</i> _{sigma} = 0.0305]	3857 [<i>R</i> _{int} = 0.0237, <i>R</i> _{sigma} = 0.0199]	4099 [<i>R</i> _{int} = 0.0291, <i>R</i> _{sigma} = 0.0233]
Data/restraints/parameters	4035/0/231	3857/0/249	4099/0/268
Goodness-of-fit on <i>F</i> ²	1.105	1.029	1.096
Final R indexes [I>=2σ (I)]	R ₁ = 0.0485, wR ₂ = 0.1366	R ₁ = 0.0309, wR ₂ = 0.0845	R ₁ = 0.0389, wR ₂ = 0.0914
Final R indexes [all data]	R ₁ = 0.0541, wR ₂ = 0.1408	R ₁ = 0.0324, wR ₂ = 0.0856	R ₁ = 0.0420, wR ₂ = 0.0931
Largest diff. peak/hole / e Å ⁻³	1.05/-0.40	0.70/-0.40	0.44/-0.38

$$R1 = \sum |F_O| - |F_C| / \sum |F_O|, wR2 = [\sum w(F_O^2 - F_C^2)^2 / \sum w(F_O^2)^2]^{1/2}$$

Table S2. Bond Lengths for 1–3.

	1		2		3	
	Atom	Atom	Length/Å	Atom	Atom	Length/Å
1¹-	Zn1	O1 ¹	1.9349(19)	Zn1	O1 ¹	1.9295(10)
	Zn1	O1	1.9349(19)	Zn1	O1	1.9295(10)
	Zn1	O3 ²	1.937(2)	Zn1	O3 ²	1.9362(10)
	Zn1	O3 ³	1.937(2)	Zn1	O3 ³	1.9362(10)
	O1	C1	1.279(4)	O2	C1	1.2204(17)
	O2	C1	1.223(3)	O1	C1	1.2746(17)
	O3	C7	1.279(3)	O3	Zn1 ²	1.9362(10)
	O4	C7	1.229(3)	O3	C7	1.2701(17)
	N1	C5	1.348(3)	O4	C7	1.2218(17)
	N1	C6	1.356(3)	N1	C5	1.3522(17)
	N1	C8	1.508(3)	N1	C6	1.3471(17)
	C1	C2	1.514(3)	N1	C8	1.06
	C2	C3	1.393(4)	N2	C21	1.142(2)
	C2	C6	1.382(4)	C1	C2	1.5200(17)
	C3	C4	1.391(4)	C2	C3	1.3833(17)
	C4	C5	1.382(4)	C2	C6	1.3788(19)
	C4	C7	1.511(4)	C3	C4	1.3911(18)
	C8	C9	1.505(4)	C4	C5	1.3764(19)
	C9	C10	1.398(4)	C4	C6	1.3763(17)
	C9	C14	1.403(4)	C8	C9	1.5018(19)
	C10	C11	1.391(4)	C9	C10	1.387(2)
	C11	C12	1.404(4)	C9	C13	1.385(2)
	C12	C13	1.400(4)	C10	C11	1.382(2)
	C12	C15	1.485(4)	C11	C12	1.388(2)
	C13	C14	1.390(4)	C12	C14	1.389(2)
	C15	C16	1.406(4)	C12	C15	1.485(2)
	C15	C20	1.403(4)	C13	C14	1.391(2)
	C16	C17	1.399(4)	C15	C16	1.391(3)
	C17	C18	1.394(5)	C15	C20	1.398(3)
	C18	C19	1.402(5)	C16	C17	1.389(3)
	C19	C20	1.395(4)	C17	C18	1.378(3)
				C18	C19	1.373(3)
				C19	C20	1.399(2)
				C20	C21	1.445(2)
				C20	C21	1.402(2)
						1.493(2)

X,+Y,1/2-Z;²¹-X,3-Y,1-Z;³+X,3-Y,-1/2+Z; **2** ¹1-X,+Y,3/2-Z;²¹-X,2-Y,1-Z;³+X,2-Y,1/2+Z

3 ¹1-X,+Y,3/2-Z;²+X,2-Y,1/2+Z;³1-X,2-Y,1-Z

Table S3. Bond Angles for Compound 1–3.

1				2				3			
Atom	Atom	Atom	Angle/ [°]	Atom	Atom	Atom	Angle/ [°]	Atom	Atom	Atom	Angle/ [°]
O1	Zn1	O1 ¹	114.78(14)	O1 ¹	Zn1	O1	112.03(6)	O1 ¹	Zn1	O1	117.73(9)
O3 ²	Zn1	O1	97.13(9)	O1 ¹	Zn1	O3 ²	120.03(5)	O1 ¹	Zn1	O3 ²	90.10(6)
O3 ³	Zn1	O1 ¹	97.13(9)	O1	Zn1	O3 ²	96.66(4)	O1	Zn1	O3 ²	122.74(7)
O3 ²	Zn1	O1 ¹	120.58(9)	O1	Zn1	O3 ³	120.03(5)	O1 ¹	Zn1	O3 ³	122.74(7)
O3 ³	Zn1	O1	120.58(9)	O1 ¹	Zn1	O3 ³	96.66(4)	O1	Zn1	O3 ³	90.10(6)
O3 ³	Zn1	O3 ²	108.09(12)	O3 ³	Zn1	O3 ²	113.07(7)	O3 ²	Zn1	O3 ³	116.72(10)
C1	O1	Zn1 ¹	123.69(18)	C1	O1	Zn1	123.70(9)	C1	O1	Zn1	124.99(12)
C7	O3	Zn1 ⁴	124.20(18)	C7	O3	Zn1 ²	128.86(9)	C5	O3	Zn1 ³	126.40(11)
C6	N1	C5	122.0(2)	C5	N1	C8	119.31(12)	C21	O5	C22	114.54(15)
C8	N1	C5	118.2(2)	C6	N1	C5	121.80(12)	C7	N1	C6	121.51(15)
C8	N1	C6	119.7(2)	C6	N1	C8	118.76(11)	C7	N1	C8	119.84(14)
O2	C1	O1	128.0(2)	O2	C1	O1	127.79(13)	C6	N1	C8	118.64(14)
C2	C1	O1	111.7(2)	O2	C1	C2	119.43(12)	O2	C1	O1	126.86(17)
C2	C1	O2	120.2(2)	O1	C1	C2	112.78(11)	O2	C1	C2	120.17(17)
C3	C2	C1	119.2(2)	C3	C2	C1	120.70(12)	O1	C1	C2	112.97(15)
C6	C2	C1	121.3(2)	C6	C2	C1	120.71(12)	C7	C2	C3	118.87(15)
C6	C2	C3	119.4(2)	C6	C2	C3	118.43(12)	C7	C2	C1	121.48(15)
C4	C3	C2	119.8(2)	C2	C3	C4	120.42(12)	C3	C2	C1	119.44(15)
C5	C4	C3	118.8(2)	C3	C4	C7	119.27(12)	C4	C3	C2	120.33(16)
C7	C4	C3	120.7(2)	C5	C4	C3	119.01(12)	C6	C4	C3	118.80(15)
C7	C4	C5	120.5(2)	C5	C4	C7	121.66(12)	C6	C4	C5	121.45(15)
C4	C5	N1	120.3(2)	N1	C5	C4	119.68(12)	C3	C4	C5	119.45(15)
C2	C6	N1	119.5(2)	N1	C6	C2	120.47(12)	O4	C5	O3	127.68(16)
O4	C7	O3	127.4(3)	O3	C7	C4	111.49(11)	O4	C5	C4	121.42(16)
C4	C7	O3	113.0(2)	O4	C7	O3	127.97(13)	O3	C5	C4	110.90(14)
C4	C7	O4	119.5(2)	O4	C7	C4	120.50(12)	N1	C6	C4	120.32(15)
C9	C8	N1	112.8(2)	N1	C8	C9	114.69(11)	N1	C7	C2	120.05(15)
C10	C9	C8	120.7(3)	C10	C9	C8	120.76(13)	N1	C8	C9	111.37(13)
C14	C9	C8	120.0(2)	C13	C9	C8	119.77(13)	C10	C9	C14	119.30(16)
C14	C9	C10	119.3(3)	C13	C9	C10	119.23(13)	C10	C9	C8	120.55(15)
C11	C10	C9	120.5(3)	C11	C10	C9	120.18(14)	C14	C9	C8	120.14(15)
C12	C11	C10	120.4(3)	C10	C11	C12	120.93(14)	C9	C10	C11	120.16(16)
C13	C12	C11	118.8(3)	C11	C12	C14	118.93(14)	C12	C11	C10	120.66(16)
C15	C12	C11	120.2(3)	C11	C12	C15	119.42(13)	C11	C12	C13	118.90(16)
C15	C12	C13	120.9(3)	C14	C12	C15	121.64(13)	C11	C12	C15	120.71(16)

C14	C13	C12	120.9(3)	C9	C13	C14	120.57(13)	C13	C12	C15	120.06(16)
C13	C14	C9	120.0(3)	C12	C14	C13	120.10(13)	C14	C13	C12	120.70(17)
C16	C15	C12	120.1(3)	C16	C15	C12	120.04(15)	C13	C14	C9	120.22(16)
C20	C15	C12	120.7(3)	C16	C15	C20	118.10(15)	C16	C15	C20	117.97(16)
C20	C15	C16	119.1(3)	C20	C15	C12	121.85(13)	C16	C15	C12	115.57(16)
C17	C16	C15	120.2(3)	C17	C16	C15	120.82(18)	C20	C15	C12	126.46(16)
C18	C17	C16	120.3(3)	C18	C17	C16	120.24(17)	C17	C16	C15	121.60(18)
C19	C18	C17	119.7(3)	C19	C18	C17	120.24(17)	C18	C17	C16	120.18(18)
C20	C19	C18	120.2(3)	C18	C19	C20	119.98(19)	C19	C18	C17	119.10(18)
C19	C20	C15	120.5(3)	C15	C20	C21	120.36(13)	C18	C19	C20	121.56(17)
				C19	C20	C15	120.61(15)	C19	C20	C15	119.53(17)
				C19	C20	C21	118.99(16)	C19	C20	C21	115.04(16)
				N2	C21	C20	178.71(17)	C15	C20	C21	125.40(15)
								O6	C21	O5	122.42(17)
								O6	C21	C20	123.13(16)
								O5	C21	C20	114.45(15)

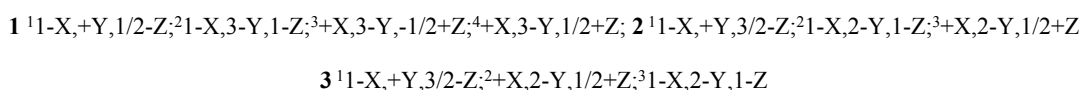
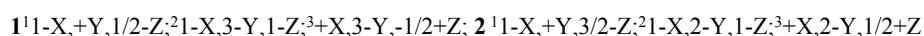


Table S4. Comparation of selected bond lengths and angles of 1–3.

Compound	Zn-O bond lengths (\AA)	O-Zn-O bond angles ($^\circ$)	N1-C8-C9 bond angles ($^\circ$)
1	Zn1-O1 1.935 Zn1-O3 1.937	O1-Zn1-O1 ¹ 114.78 O3 ² -Zn1-O1 97.13 O3 ³ -Zn1-O1 ¹ 97.13	112.8
		O3 ² -Zn1-O1 ¹ 120.58	
		O3 ³ -Zn1-O1 120.58	
	Zn1-O1 1.930 Zn1-O3 1.936	O3 ³ -Zn1-O3 ² 123.69 O1-Zn1-O1 ¹ 112.03 O3 ² -Zn1-O1 96.66	114.7
		O3 ³ -Zn1-O1 ¹ 96.99	
		O3 ² -Zn1-O1 ¹ 120.03	
2	Zn1-O1 1.930 Zn1-O3 1.936	O3 ³ -Zn1-O1 120.03 O3 ³ -Zn1-O3 ² 113.07 O1-Zn1-O1 ¹ 117.73	111.4
		O3 ² -Zn1-O1 90.10	
		O3 ³ -Zn1-O1 ¹ 90.10	
	Zn1-O1 1.931 Zn1-O3 1.933	O3 ² -Zn1-O1 122.74	111.4
		O3 ³ -Zn1-O1 122.74	
		O3 ³ -Zn1-O3 ² 116.72	



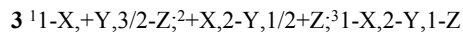


Table S5. The fitting parameters of the lifetime of 1–3.

Compound	Tempera ture(K)	λ_1 (nm)	λ_2 (nm)	τ_1 (ns) ^a	τ_2 (ms) ^b
L1	298	397	/	2.88(19.37%)	/
)	8.97(80.63%)	/
L2	298	404	/	1.44(37.97%)	/
			/	4.84(62.03%)	/
L3	298	437		4.04(12.18%)	
				13.04(87.82%)	
1	100	411	573	1.01(23.11%)	10.90(4.40%)
				3.30(55.08%)	147.20(28.43%)
				12.20(21.80%)	501.60(67.17%)
2	298	420	580	0.83(21.19%)	0.84(9.11%)
				3.25(45.70%)	4.10(18.37%)
				12.65(33.10)	16.92(72.52%)
3	298	450	570	1.94(61.64%)	0.70(8.98%)
				9.25(38.36%)	2.69(30.44%)
				10.39(27.69%)	
3	298	450	605	0.73(58.54%)	1.07(39.19%)
				2.46(41.46%)	4.84(31.08%)
				19.37(17.60%)	
^a The				144.5(12.13%)	

lifetime corresponding to the λ_1 . ^bThe lifetime corresponding to the λ_2 .

Table S6. The comparision of cell parameters before and after structural optimizations.*

	1		2		3	
	expt	opt	expt	opt	expt	opt
<i>a</i> / Å	28.723	28.723	28.420	28.420	31.265	31.264
<i>b</i> / Å	7.883	7.883	8.408	8.408	8.071	8.071
<i>c</i> / Å	14.575	14.568	14.546	14.546	14.877	14.876
α	90.00	90.00	90.00	90.00	90.00	90.00
β	91.79	91.79	96.86	96.86	103.09	103.09
γ	90.00	90.00	90.00	90.00	90.00	90.00
<i>V</i> / Å ³	3298.5	3298.4	3450.6	3450.6	3656.5	3656.5

*Since there is no obvious change before and after structural optimizations, the optimized crystallographic data were adopted for all calculations.

References

1. Kresse, G.; Furthmüller, J. Efficiency of Ab-Initio Total Energy Calculations for Metals and Semiconductors Using a Plane-Wave Basis Set. *Comp. Mater . Sci.* 1996, **6**, 15-50.
2. Perdew, J. P .; Burke, K.; Ernzerhof, M. Generalized Gradient Approximation Made Simple. *Phys. Rev. Lett.* 1996, **77**, 3865-3868.
3. Kresse, G.; Joubert, D. From Ultrasoft Pseudopotentials to the Projector Augmented-Wave Method. *Phys. Rev. B* 1999, **59**, 1758-1775.
4. Grimme, S.; Antony, J.; Ehrlich, S.; Krieg, H. A Consistent and Accurate Ab Initio Parametrization of Density Functional Dispersion Correction (DFT-D) for the 94 Elements H-Pu. *J. Chem. Phys.* 2010, **132**, 154104.
5. V. Wang, Y.-Y. Liang, Y. Kawazeo, W.-T. Geng, High-Throughput Computational Screening of Two-Dimensional Semiconductors, arXiv:1806.04285.